Stability of Reaction on a Spherical Particle

D. K. WINEGARDNER and R. A. SCHMITZ

University of Illinois, Urbana, Illinois

This paper presents a theoretical study of the stability of chemical reaction on the external surface of a single spherical particle in stagnant surroundings. The analysis, which invokes methods of linear stability theory, yields necessary and sufficient conditions for stability of a steady state solution to small disturbances for the cases of very small and very large solid thermal conductivity. It is shown that heat losses from the solid surface may lead to transient behavior which is characteristically different from that for adiabatic surfaces, and that the unsteady state is strongly affected by the thermal capacity of the solid material. A numerical example is employed to illustrate the possible significance of unstable situations.

Presented here is an analytical study of the stability of the steady state of a distributed parameter heterogeneous reaction system which comprises a single, nonporous, spherical particle in an infinite, stagnant expanse of reactants. Although considerably idealized for mathematical tractability, the physical model contains many of the essential features of real systems, so that the results should provide some theoretical insight into the behavior, at least as a low Reynolds number limit, of more complicated situations such as those encountered in catalytic reactors and catalyst regeneration and particulate burning processes.

A theoretical study of a problem very similar to that considered here has been reported by Petersen and coworkers (*1, 2*) who were primarily concerned with the effects of an unsymmetric state of the fluid at an infinite distance from the solid surface. Their studies of a single-step reaction involving a single reactant pointed out the existence of three steady state solutions in some cases and, by means of a modified Nyquist method, showed that the intermediate state was unstable to small disturbances. In the present study the state of the fluid infinitely far from the solid surface is assumed to be uniform, but otherwise the analysis is based on a more general mathematical description than that of the above references and yields a more complete elucidation of the nature of the transient state.

The stability of porous catalyst particles with internal diffusion and reaction and with negligible external resistance to transport has been treated by Amundson and co-workers (*3, 4*).

THE PHYSICAL MODEL

A single reaction of the general form

$$\sum_{j=1}^{n} a_j A_j = 0 \qquad (1)$$

is assumed to occur on the external surface of the spherical particle. In Equation (1) the stiochiometric coefficients a_j are positive for reactants, negative for products, and zero for inert substances. The mathematical description in the following section is intended to apply, at least to a first approximation, to the case of a catalytic reaction occurring on a nonreacting solid or of a solid particle which is reacting at its surface with the external fluid such as might be assumed in heterogeneous burning. In addition to the assumption of no bulk fluid motion, a number of other simplifying assumptions are made throughout the study for analytic convenience. These include equal component diffusivities in the fluid mixture, a Lewis number of unity, constant density and diffusivity for the fluid, constant state of the external fluid at an infinite distance from the solid particle, no net material flow to or from the solid surface, and quasi steady particle size and/or catalytic activity.

MATHEMATICAL DESCRIPTION

Under the assumptions listed above, a material balance on components in the fluid phase may be written as

$$\frac{\partial \mathbf{x}}{\partial \tau} = \nabla^2 \mathbf{x} \quad (\eta > 1) \qquad (2)$$

Energy balances on the fluid and solid phases yield

$$\frac{\partial H}{\partial \tau} = \nabla^2 H \quad (\eta > 1) \tag{3}$$

$$\frac{\partial T^*}{\partial \tau} = L\nabla^2 T^* \quad (0 < \eta < 1) \tag{4}$$

where

$$H = \sum_{j=1}^{n} x_j h_j \tag{5}$$

and

$$h_j = h_j^o + \int_{T^o}^{T} C_{pj}\, dT \tag{6}$$

As a result of the simplifying assumptions, the material and energy balances above are linear. All nonlinearities are confined to the boundary conditions which are given by

$$T^*(0, \theta, \phi, \tau), \text{ finite} \tag{7}$$

$$\left.\begin{aligned} \frac{\partial \mathbf{x}}{\partial \eta}(1, \theta, \phi, \tau) &= -\mathbf{a}R[\mathbf{x}(1, \theta, \phi, \tau), T(1, \theta, \phi, \tau)] \\ \frac{\partial H}{\partial \eta}(1, \theta, \phi, \tau) - K\frac{\partial T^*}{\partial \eta}(1, \theta, \phi, \tau) &= Q[T(1, \theta, \phi, \tau)] \\ T(1, \theta, \phi, \tau) &= T^*(1, \theta, \phi, \tau) \end{aligned}\right\} \tag{8}$$

$$\left.\begin{aligned} \mathbf{x}(\infty, \theta, \phi, \tau) &= \mathbf{x}_\infty \\ H(\infty, \theta, \phi, \tau) &= H_\infty \end{aligned}\right\} \tag{9}$$

The function Q in Equation (8) accounts for nonadiabaticity of the solid surface, particularly for radiation losses to the surroundings.

Linearized Equations

Equations (2), (3), and (4) may be written in terms of perturbation variables as follows:

$$\frac{\partial \mathbf{p}}{\partial \tau} = \nabla^2 \mathbf{p} \quad (\eta > 1) \tag{10}$$

$$\frac{\partial p^*}{\partial \tau} = L\nabla^2 p^* \quad (\eta < 1) \tag{11}$$

where p^* and the vector $\mathbf{p}$ represent disturbances from the steady state of the system. Thus

$$p^* = T - T_s \tag{12}$$

$$\mathbf{p} = \begin{pmatrix} x_1 - x_{1,s} \\ \vdots \\ x_n - x_{n,s} \\ H - H_s \end{pmatrix} \tag{13}$$

If attention is restricted to small disturbances from a steady state, it is reasonable to assume that the transients are suitably described by the solutions of Equations (10) and (11) subjected to linearized forms of the boundary conditions. Linearization yields

$$R(\mathbf{x}, T) \cong R(\mathbf{x}_s, T_s) + \sum_{i=1}^{n}\left(\frac{\partial R}{\partial x_i}\right)_s (x_i - x_{i,s}) + \left(\frac{\partial R}{\partial T}\right)_s (T - T_s)$$

$$Q(T) \cong Q(T_s) + \left(\frac{\partial Q}{\partial T}\right)_s (T - T_s)$$

Also, from Equations (5) and (6)

$$H(\mathbf{x}, T) \cong H(\mathbf{x}_s, T_s) + \sum_{i=1}^{n}\left(\frac{\partial H}{\partial x_i}\right)_s (x_i - x_{i,s}) + \left(\frac{\partial H}{\partial T}\right)_s (T - T_s) \tag{14}$$

By means of Equations (12), (13), and (14), the boundary conditions in Equations (7), (8), and (9) may be written in the following form:

$$p^*(0, \theta, \phi, \tau), \text{ finite} \tag{15}$$

$$\left.\begin{aligned} \frac{\partial \mathbf{p}}{\partial \eta}(1, \theta, \phi, \tau) &= \mathbf{A}\, p(1, \theta, \phi, \tau) + \mathbf{B}\frac{\partial p^*}{\partial \eta}(1, \theta, \phi, \tau) \\ \mathbf{C}\ \mathbf{p}(1, \theta, \phi, \tau) &= p^*(1, \theta, \phi, \tau) \end{aligned}\right\} \tag{16}$$

$$\mathbf{p}(\infty, \theta, \phi, \tau) = \mathbf{0} \tag{17}$$

where **A**, **B**, and **C** are the following matrices:

$$\mathbf{A} = \begin{pmatrix} -a_1\left(\frac{\partial R}{\partial x_1}\right) & \cdots & -a_1\left(\frac{\partial R}{\partial x_n}\right) & -a_1\left(\frac{\partial R}{\partial T}\right) \\ \vdots & & & \\ -a_n\frac{\partial R}{\partial x_1} & \cdots & -a_n\frac{\partial R}{\partial x_n} & -a_n\frac{\partial R}{\partial T} \\ 0 & \cdots & 0 & \frac{\partial Q}{\partial T} \end{pmatrix}_s \times \begin{pmatrix} 1 & \cdots & 0 & 0 \\ \vdots & & \vdots & \vdots \\ 0 & \cdots & 1 & 0 \\ \frac{-\partial H/\partial x_1}{\partial H/\partial T} & \cdots & \frac{\partial H/\partial x_n}{\partial H/\partial T} & \frac{1}{\partial H/\partial T} \end{pmatrix}_s \tag{18}$$

$$\mathbf{B} = \begin{pmatrix} 0 \\ \vdots \\ 0 \\ K \end{pmatrix} \quad (n+1 \text{ order}) \tag{19}$$

$$\mathbf{C} = \begin{pmatrix} \frac{-\partial H/\partial x_1}{\partial H/\partial T} & \cdots & \frac{-\partial H/\partial x_n}{\partial H/\partial T} & \frac{1}{\partial H/\partial T} \end{pmatrix}_s \tag{20}$$

It is noted here that all entries in the matrices **A**, **B**, and **C** are to be evaluated at the steady state. Furthermore, they are independent of position since they are evaluated at the particle surface in Equation (16). Thus the matrices are assumed to be known from solution of the governing steady state equations.

STABILITY ANALYSIS

The Eigenvalue Problem

Separable solutions of the $n + 2$ linearized transient equations given in Equations (10) and (11) may be ex-

pressed in terms of spherical harmonics (5) in the form

$$\begin{pmatrix} \mathrm{p} \\ p^* \end{pmatrix} = [P^m{}_l(\cos\theta)\ e^{\pm im\phi}]e^{\lambda\tau}\begin{pmatrix} \mathbf{f}\ (\eta, l, \lambda) \\ f^*\ (\eta, l, \lambda) \end{pmatrix} \quad (21)$$

The wave numbers l and m in Equation (21) are nonnegative integers. The necessary and sufficient condition for stability to small disturbances is that the eigenvalue λ have negative real parts. The eigenvalue problem, formulated by substitution from Equation (21) into Equations (10), (11), (15), (16), and (17), is represented by the following homogeneous system:

$$\frac{d^2\mathbf{f}}{d\eta^2} + \frac{2}{\eta}\frac{d\mathbf{f}}{d\eta} - \left[\frac{l(l+1)}{\eta^2} + \lambda\right]\mathbf{f} = \mathbf{0} \quad (22)$$

$$\frac{d^2f^*}{d\eta^2} + \frac{2}{\eta}\frac{df^*}{d\eta} - \left[\frac{l(l+1)}{\eta^2} + \frac{\lambda}{L}\right]f^* = 0 \quad (23)$$

$$f^*\ (0, l, \lambda), \text{ finite} \quad (24)$$

$$\left.\begin{aligned} \frac{d\mathbf{f}}{d\eta}(1, l, \lambda) &= \mathbf{A}\,\mathbf{f}(1, l, \lambda) + \mathbf{B}\frac{df^*}{d\eta}(1, l, \lambda) \\ \mathbf{C}\mathbf{f}(1, l, \lambda) &= f^*(1, l, \lambda) \end{aligned}\right\} \quad (25)$$

$$\mathbf{f}(\infty, l, \lambda) = \mathbf{0} \quad (26)$$

As shown by the above system of equations, the eigenvalue problem is independent of the wave number m.

General solutions to the uncoupled system of second-order differential equations above may be expressed in terms of modified Bessel functions as follows:

$$\mathbf{f}(\eta, l, \lambda) = \alpha\frac{I_{l+1/2}(\sqrt{\lambda}\,\eta)}{(\sqrt{\lambda}\,\eta)^{1/2}} + \beta\frac{I_{-(l+1/2)}(\sqrt{\lambda}\,\eta)}{(\sqrt{\lambda}\,\eta)^{1/2}} \quad (27)$$

$$f^*(\eta, l, \lambda) = \alpha^*\frac{I_{l+1/2}\left(\sqrt{\frac{\lambda}{L}}\,\eta\right)}{\left(\sqrt{\frac{\lambda}{L}}\,\eta\right)^{1/2}} + \beta^*\frac{I_{-(l+1/2)}\left(\sqrt{\frac{\lambda}{L}}\,\eta\right)}{\left(\sqrt{\frac{\lambda}{L}}\,\eta\right)^{1/2}} \quad (28)$$

The Spectrum of λ

Certain information regarding the spectrum of the eigenvalue λ may be gleaned from the asymptotic form of the solution given by Equation (27). For large values of η, the modified Bessel functions approach the following relationships (6):

$$\frac{I_{l+1/2}(\sqrt{\lambda}\,\eta)}{(\sqrt{\lambda}\,\eta)^{1/2}} \sim -i\sqrt{\frac{2}{\pi}}\frac{e^{-i\,l\pi/2}}{\sqrt{\lambda}\,\eta}\cos[i\sqrt{\lambda}\,\eta - (l+1)\pi/2] \quad (29)$$

$$\frac{I_{-(l+1/2)}(\sqrt{\lambda}\,\eta)}{(\sqrt{\lambda}\,\eta)^{1/2}} \sim -i\sqrt{\frac{2}{\pi}}\frac{e^{i(l+1)\,3\pi/2}}{\sqrt{\lambda}\,\eta}\sin[i\sqrt{\lambda}\,\eta - (l+1)\,\pi/2] \quad (30)$$

Consider first the admissibility of negative real values of λ. In this case $\mathbf{f}(\eta, l, \lambda)$ in Equation (27) approaches zero for large values of η independently of the values of α and β because the expressions in Equations (29) and (30) both approach zero. Thus, condition (26) is always satisfied if λ is real and negative, and, as a result, it provides no information to aid in determining the constants α and β. Substitution then from Equations (27) and (28) into Equation (25) and consideration of the finiteness condition in Equation (24) will lead to a set of $n + 3$ linear algebraic equations for the $2n + 4$ coefficients. Consequently, nontrivial solutions to the system (22) through (26) are obtainable for any real negative value of λ; that is, the spectrum includes a continuous portion along the negative real axis in the complex λ plane.

In addition to the continuum, the spectrum of λ may include discrete points, not on the negative real axis, in the complex λ plane. For complex or real positive eigenvalues, the modified Bessel functions approach the following relationships for large values of η:

$$\frac{I_{l+1/2}(\sqrt{\lambda}\,\eta)}{(\sqrt{\lambda}\,\eta)^{1/2}} \sim \left(\frac{Re\,(\sqrt{\lambda})}{|Re\,(\sqrt{\lambda})|}\right)^{l+1}\frac{e^{|\sqrt{\lambda}|\,\eta}}{\sqrt{2\pi\,\lambda}\,\eta} \quad (31)$$

$$\frac{I_{-(l+1/2)}(\sqrt{\lambda}\,\eta)}{(\sqrt{\lambda}\,\eta)^{1/2}} \sim \left(\frac{Re\,(\sqrt{\lambda})}{|Re\,(\sqrt{\lambda})|}\right)^{l}\frac{e^{|\sqrt{\lambda}|\,\eta}}{\sqrt{2\pi\,\lambda}\,\eta} \quad (32)$$

Both of the above expressions approach infinity as η becomes large, and, as a result, Equation (26) can be satisfied if and only if

$$\beta = -\frac{|Re\,(\sqrt{\lambda})|}{Re\,(\sqrt{\lambda})}\,\alpha \quad (33)$$

Furthermore, the condition of finiteness on $f^*(\eta, l, \lambda)$ requires that β^* in Equation (28) be zero. This fact together with the relationship in Equation (33) leads, upon substitution from Equations (27) and (28) into Equation (25), to a system of $n + 2$ linear homogeneous algebraic equations for α^* and the $n + 1$ components of α. A demand that the coefficient matrix be singular to insure nontrivial solutions produces the following characteristic equations:

$$V(\lambda, l) = 0 \quad (34)$$

and

$$\Gamma_2 - [\Gamma_1 - 2V(\lambda, l)]^2 + 4\Gamma_4\, v(\lambda, l, L)\,[\Gamma_3 + V(\lambda, l)] = 0 \quad (35)$$

where, by employing some Bessel function identities, $V(\lambda, l)$ and $v(\lambda, l, L)$ may be expressed as

$$\left.\begin{aligned} V(\lambda, l) &= \sqrt{\lambda}\times\left[\frac{|Re\,(\sqrt{\lambda})|\,I_{l-1/2}(\sqrt{\lambda}) - Re\,(\sqrt{\lambda})\,I_{-(l-1/2)}(\sqrt{\lambda})}{|Re\,(\sqrt{\lambda})|\,I_{l+1/2}(\sqrt{\lambda}) - Re\,(\sqrt{\lambda})\,I_{-(l+1/2)}(\sqrt{\lambda})}\right] - (l+1) \\ v(\lambda, l, L) &= \sqrt{\frac{\lambda}{L}}\frac{I_{l-1/2}(\sqrt{\lambda/L})}{I_{l+1/2}(\sqrt{\lambda/L})} - (l+1) \end{aligned}\right\} \quad (36)$$

Γ_1, Γ_2, Γ_3, and Γ_4 in Equation (35) are scalar groups of constants derived from the matrices **A**, **B**, and **C** as follows:

$$\Gamma_1 = tr\ \mathbf{A} \quad (37)$$

$$\Gamma_2 = (\Gamma_1 - 2)^2 - 4\ \det(\mathbf{I} - \mathbf{A}) \quad (38)$$

$$\Gamma_3 = -\Gamma_1 + (\mathbf{C}\cdot\mathbf{A}\cdot\mathbf{B})/(\mathbf{C}\cdot\mathbf{B}) = \sum_{i=1}^{n} a_i\frac{\partial R(\mathbf{x}, T)}{\partial x_i} \quad (39)$$

$$\Gamma_4 = \mathbf{C}\cdot\mathbf{B} = k_t^*/k_t \quad (40)$$

It may be shown that Equation (34) cannot be satisfied by any complex or real positive value of λ. Perhaps the simplest way of proving this is to examine the roots of

Equation (35) for the particular case of Γ_1, Γ_2, and Γ_4 all equal to zero, since then Equations (34) and (35) are identical. This examination will be carried out in the next section.

Equation (35) thus defines the discrete portion of the spectrum of λ, if such a portion exists. Since it is only the discrete portion that contains any complex or real positive eigenvalues, only the λ's resulting from Equation (35) can lead to unstable behavior and oscillatory responses. It is understood that in all cases for all values of the parameters there exists, in addition to the contribution from any discrete eigenvalues, a time-decaying contribution to the transient solution from the continuous portion of the spectrum of λ.

In accordance with Equation (35), a general study of the eigenvalues would involve consideration of the effects of five parameters, namely, Γ_1, Γ_2, Γ_3, Γ_4, and L. For given values of these quantities, a numerical investigation of the roots of Equation (35) would be rather straightforward. However, the large number of parameters would make a general parametric study of Equation (35) awkward and fruitless as far as gaining any theoretical insight is concerned. Two limiting forms of Equation (35), in particular those for very small and very large values of Γ_4, are amendable to detailed study and will be considered in subsequent sections.

Stability Criteria for the Case of Negligible Solid Thermal Conductivity

A particularly simple form of Equation (35) results if the thermal conductivity of the solid material is assumed to be vanishingly small. This is perhaps a poor assumption in general; it implies that the solid material itself is of no consequence in the transient behavior of the reaction process. In this idealization, the particle merely provides a surface for reaction and permits no conduction of heat through or around the surface. The mathematical simplification that results by virtue of the assumption permits a thorough study of the eigenvalues and provides a basis for more general analyses of Equation (35). It will be shown in the next section that the convenient and simple criteria for stability resulting here are at least sufficient in the more realistic case of a large solid thermal conductivity.

With $\Gamma_4 = 0$. Equation (35) reduces to

$$\Gamma_2 - [\Gamma_1 - 2V(\lambda, l)]^2 = 0 \qquad (41)$$

For a fixed value of l, and with λ represented by $\bar{a} + i\bar{b}$, where $\bar{a}$ and $\bar{b}$ are given real constants, Equation (41) with $V(\lambda, l)$ computed from Equation (36) will yield a locus of points in the (Γ_1, Γ_2) plane. Regions of stable and unstable behavior, for that particular value of l, may be located by computing the loci of marginal states. These states, which separate stable from unstable responses, are obtained by taking $\bar{a} = \bar{b} = 0$ (marginal stationary states) and also by taking $\bar{a} = 0$, $\bar{b} \neq 0$ (marginal oscillatory states).

Consider first the case of real eigenvalues and marginal stationary states. It follows from Equation (41) that Γ_2 is positive, and from Equation (36) it may be shown that

$$V(0, l) = -(l + 1)$$

Thus the marginal stationary states are given by

$$\Gamma_2 = [\Gamma_1 + 2(l + 1)]^2 \qquad (42)$$

which describes the family of parabolas shown in Figure 1. The parabolas all have vertices on the Γ_1 axis and continue to shift to the left in Figure 1 as l is increased. It may be shown by computations from Equation (41) with real, positive, and nonzero values of λ that real positive eigenvalues, thus unstable states, exist in that region which lies above the Γ_1 axis and to the left of the right arm of the parabola for a given value of l. Furthermore, for any point lying within a parabola for a given value of l there exists one positive eigenvalue for that particular l, while for any point to the left of that parabola a pair of distinct positive eigenvalues exists.

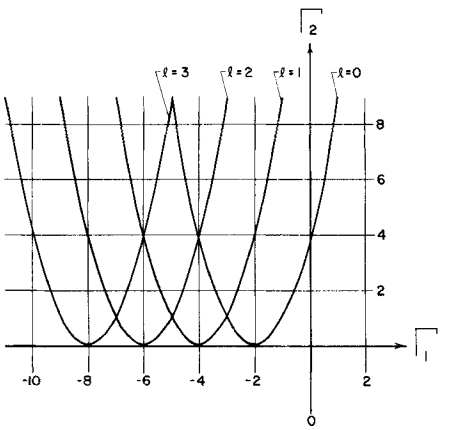

Fig. 1. Marginal stationary states.

Clearly the stability of a steady state requires its stability to all wave numbers; instability will follow from its instability to even one value of l. Thus it follows that a necessary condition for stability is that the point Γ_1, Γ_2, as computed from Equations (37) and (38) with the matrix A given by Equation (18), lie to the right of the parabola for $l = 0$ in Figure 1. From Equation (42) this condition may be expressed as

$$\Gamma_1 > \sqrt{\Gamma_2} - 2 \quad \text{for} \quad \Gamma_2 < 0 \qquad (43)$$

It will be clear shortly that this is not only a necessary but also a sufficient condition for stability providing $\Gamma_2 > 0$. Consideration of complex eigenvalues will lead to another condition for $\Gamma_2 < 0$.

Marginal oscillatory states are generated in a similar manner, by considering λ to be purely imaginary. For these states then Equation (41) gives

$$\Gamma_1 = 2\ Re\,[V(i\bar{b}, l)] \qquad (44)$$

$$\Gamma_2 = -4\,\{Im\,[V(i\bar{b}, l)]\}^2 \qquad (45)$$

It follows from Equation (45) that Γ_2 is always negative, and thus the sufficiency of condition (43) for positive values of Γ_2 is established.

Loci of marginal oscillatory states as computed from Equations (36), (44), and (45) are shown as the solid curves in Figure 2. The curves continue to shift to the left as l is increased beyond those values shown in the figure, and all curves converge to the curve for $l = 0$ as $\Gamma_2 \to -\infty$. Here as before stability must be insured for all values of l. Computations from Equations (36) and (41) with the real part of λ taken to be positive and the imaginary part nonzero establish the fact that to the left of the solid line for a given value of l in Figure 2 there exists a pair of complex conjugate eigenvalues with a positive real part. Thus all states to the left of the solid curve for $l = 0$ are unstable and should exhibit an oscillatory response with the amplitude of the oscillations increasing with time. The locus of marginal states for $l = 0$ may be expressed in a convenient analytical form. From Equa-

tion (36) it may be shown that

$$V(\lambda, 0) = -\sqrt{\lambda}\frac{Re\,(\sqrt{\lambda})}{|Re\,(\sqrt{\lambda})|} - 1 \qquad (46)$$

If $\sqrt{\lambda} = a + ib$, then from Equations (46) and (47)

$$\Gamma_1 = -2\,(|a| + 1) \qquad (47)$$

$$\Gamma_2 = -4b^2 \qquad (48)$$

Now for the marginal oscillatory states, $\bar{a} = 0$, or $a = \pm b$, and from Equations (47) and (48)

$$\Gamma_1 = -(\sqrt{-\Gamma_2} + 2) \qquad (49)$$

Thus for stability

$$\Gamma_1 > -\sqrt{-\Gamma_2} - 2 \quad \text{for} \quad \Gamma_2 < 0 \qquad (50)$$

Inequalities (43) and (50) thus constitute necessary and sufficient conditions for stability of a steady state to small disturbances.

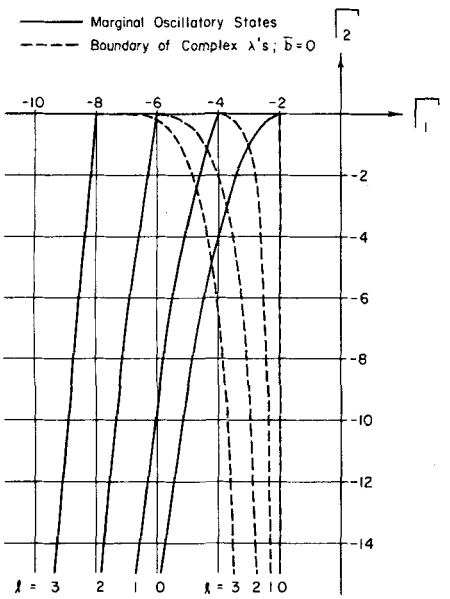

Fig. 2. Marginal oscillatory states.

It is of interest also to establish the bounds, in the (Γ_1, Γ_2) plane, of the domain of complex eigenvalues, that is, of oscillatory responses. For $l = 0$, these bounds are given by Equations (47) and (48) with a or b equal to zero. With $a = 0$, there results a vertical line at $\Gamma_1 = -2$ in the lower half of the plane and with $b = 0$ a straight line extending from -2 to infinity along the Γ_1-axis. For other values of l such bounds were computed from Equation (41) by letting b approach zero. For any given value of l one bound is a ray extending to the left along the Γ_1 axis and beginning at the point of intersection of the locus of marginal oscillatory states for that l and the Γ_1 axis. The right-hand bounds are shown as the dashed curves in Figure 2. For a particular value of l a pair of complex conjugate eigenvalues exists for every point to the left of the dashed curve for that value of l and below the Γ_1 axis. For those points lying between the dashed curve and the locus of marginal oscillatory states for a given value of l the real part of the pair of complex conjugates is negative.

The results of this section may be summarized conveniently by dividing the (Γ_1, Γ_2) plane into four regions as shown in Figure 3. Throughout region I in that figure all states are stable and nonoscillatory; only a continuum of negative real eigenvalues exists. In region II at least one real positive eigenvalue exists, and a disturbance from a steady state will eventually grow in an exponential manner. Points in region III yield at least one pair of complex conjugate eigenvalues with a positive real part. A disturbance from a steady state in this region would lead to an oscillatory response with amplitude increasing with time. The response to small disturbances will also be oscillatory in nature for steady states in region IV; however, since the complex eigenvalues there have negative real parts, the amplitudes will decay with time. By means of Figure 3, or through conditions (43) and (50) with Γ_1 and Γ_2 computed from Equations (18), (37), and (38), stability or instability of a steady state may be ascertained once the steady state at the particle surface is known.

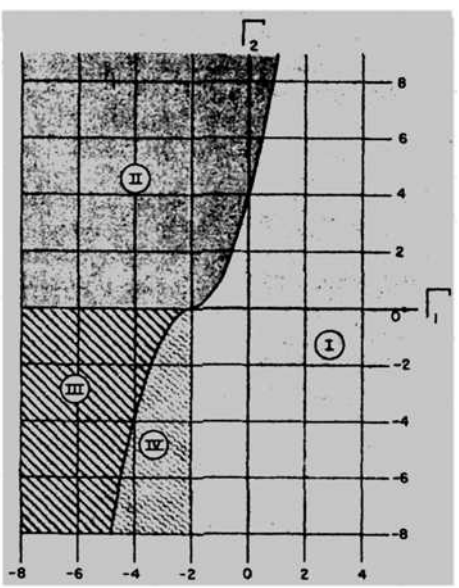

Fig. 3. Results of stability analysis for negligible solid thermal conductivity.

A statement made earlier to the effect that no complex or positive real eigenvalues are contributed by Equation (34) may now be confirmed with the aid of Figure 3. The roots of Equation (34) for a given value of l are just those from Equation (41) with Γ_1 and Γ_2 equal to zero. Thus the nature of the roots of Equation (35) is characterized by the origin in Figure 3 which is seen to lie in region I where only the continuum of negative λ's exists.

One further noteworthy point may be made in this section regarding the effect of heat losses from the surface. If Q in Equation (8) is zero (the case of an adiabatic surface as studied in references *1* and *2*), it may be shown from Equations (18) and (39) that all states must lie on the parabola

$$\Gamma_2 = \Gamma_1^2 \qquad (51)$$

in the (Γ_1, Γ_2) plane. As a result all states in this case lie in either regions I or II of Figure 3, and no oscillatory responses are possible.

Stability Criteria for the Case of Large Solid Thermal Conductivity

In the previous case of negligible solid thermal conductivity, no properties of the solid material were involved

in the characteristic equation. In the present section a more realistic extreme, that of a large thermal conductivity, will be considered. This case permits an investigation of the effects of the solid heat capacity on the transient state.

The assumption of an infinite thermal conductivity implies that the temperature may be considered to be uniform throughout the solid material as well as over its surface at all times.

By means of Equations (36) and (40) the following limits may be established:

$$\lim_{k_t^* \to \infty} [\Gamma_4 v(\lambda, l, L)] = \begin{cases} \frac{\lambda}{3}\omega & \text{for } l = 0 \\ \infty & \text{for } l \neq 0 \end{cases} \quad (52)$$

Accordingly, for $l \neq 0$, Equation (35) can be satisfied if and only if the quantity $[\Gamma_3 + V(\lambda, l)]$ vanishes. That this is generally impossible and hence that no discrete eigenvalues are possible for $l \neq 0$ may be established by means of the following arguments. It is pointed out first that Γ_3 is usually negative because the two factors a_i and $\partial R(\mathbf{x}, T)/\partial x_i$ in each term of Equation (39) are of opposite sign; at least this is true for reaction rates which obey the law of mass action. It does not appear to be necessarily true in the special cases of autocatalytic reactions and of reactions in which a reactant retards the forward rate. The assumption will be made here that $\Gamma_3 < 1$. From Equation (36) it may be shown that $V(\lambda, l) < -1$. Thus the quantity $[\Gamma_3 + V(\lambda, l)]$ cannot vanish, and nonzero values of l in Equation (35) need not be considered. This means that if the solid has a large thermal conductivity, any nondecaying contribution to the transient response will grow symmetrically. Also, any oscillatory contribution to the response will be symmetric.

From these arguments and with substitution from Equations (52) and (46), the characteristic equation to be studied here may be written as

$$\Gamma_2 + \frac{4}{3}\omega\lambda\left[\Gamma_3 - \sqrt{\lambda}\frac{Re(\sqrt{\lambda})}{|Re(\sqrt{\lambda})|} - 1\right] = \left[\Gamma_1 + 2\sqrt{\lambda}\frac{Re(\sqrt{\lambda})}{|Re(\sqrt{\lambda})|} + 2\right]^2 \quad (53)$$

For $\omega = 0$, such as in the special case of a negligible solid heat capacity, Equation (53) reduces to Equation (41) with $l = 0$. Thus the arguments regarding the eigenvalue problem for $l = 0$ in the previous section apply. The necessary and sufficient conditions for stability for this case are given by Equations (43) and (50), and the transient description is summarized in Figure 3. That figure will be used as a basis for presenting in subsequent considerations the effect of ω which characterizes the effect of solid volumetric heat capacity $\rho^* C_p^*$.

It can be seen from Equation (53) that the locus of marginal stationary states is independent of ω. That locus, obtained from Equation (53) by setting $\lambda = 0$, is given by Equation (42) with $l = 0$ and is shown as the parabola in the upper half of the (Γ_1, Γ_2) plane of Figure 1.

The second term on the left of Equation (53) and thus the solid heat capacity does play a role, however, in establishing the locus of marginal oscillatory states and the domain of complex eigenvalues in the (Γ_1, Γ_2) plane.

As before, consider the complex form of λ as

$$\sqrt{\lambda} = a + ib \quad (54)$$

or

$$\lambda = a^2 - b^2 + 2abi \quad (55)$$

Substitution from Equation (54) into Equation (53) leads to the following parametric equations which must be satisfied by any complex eigenvalue:

$$\Gamma_2 + \frac{4}{3}\omega[(a^2 - b^2)(\Gamma_3 - |a| - 1) + 2|a|b^2] = [(\Gamma_1 + 2) + 2|a|]^2 - 4b^2 \quad (56)$$

$$(\Gamma_1 + 2) + 2|a| = -\frac{\omega}{3}[(a^2 - b^2) - 2|a|(\Gamma_3 - |a| - 1)] \quad (57)$$

From Equations (56) and (57), relationships for the loci of marginal oscillatory states and for points on the bounds of the domain of complex eigenvalues may be extracted. While in the case of negligible solid conductivity these loci depend only on the parameter groups Γ_1 and Γ_2, they will be seen here to depend in addition on Γ_3 and ω.

Consider first the bounds of the domain of complex λ's. Here the imaginary part of λ in Equation (55) vanishes; that is, $a = 0$ or $b = 0$. With $a = 0$ and b eliminated between Equations (56) and (57) there results

$$\Gamma_1 + 2 = 2\left[\frac{3}{\omega} + (1 - \Gamma_3)\right] \pm \sqrt{4\left[\frac{3}{\omega} + (1 - \Gamma_3)\right]^2 + \Gamma_2} \quad \text{for } \Gamma_1 + 2 \geq 0 \quad (58)$$

For a given value of the quantity $\left(\frac{3}{\omega} - \Gamma_3\right)$, Equation (58) describes a section of a parabola in the (Γ_1, Γ_1) plane which begins on the Γ_1 axis at -2 and has its vertex at the point $\Gamma_1 = 2\left(\frac{3}{\omega} - \Gamma_3\right)$, $\Gamma_2 = -4\left[\frac{3}{\omega} + (1 - \Gamma_3)\right]^2$. For a given value of Γ_3 the locus in the (Γ_1, Γ_2) plane is contained in a region bounded by the asymptotic forms of Equation (58) for $\omega \to 0$, as for a very small solid heat capacity, and for $\omega \to \infty$, as for a very large capacity. As ω approaches zero, the locus given by Equation (58) approaches a vertical line at $\Gamma_1 = -2$. As ω approaches infinity, on the other hand, it approaches a portion of a parabola given by

$$\Gamma_1 + 2 = 2(1 - \Gamma_3) \pm \sqrt{4(1 - \Gamma_3)^2 + \Gamma_2}\,; \quad \Gamma_1 + 2 \geq 0 \quad (59)$$

The effect of increasing ω then is to shrink region I of Figure 3. As Γ_3 approaches unity, the locus of points in the (Γ_1, Γ_2) plane given by Equation (59) becomes coincident with the right boundary of region II in Figure 3 to eliminate entirely region I.

The other bound on the domain of complex eigenvalues is obtained from Equations (56) and (57) with $b = 0$. In this case there results the following parametric equations:

$$\Gamma_2 - [(\Gamma_1 + 2) + 2|a|]^2 = -\frac{4}{3}\omega a^2(\Gamma_3 - |a| - 1) \quad (60)$$

$$(\Gamma_1 + 2) + 2|a| = \frac{2|a|}{2}\omega\left(\Gamma_3 - \frac{3|a|}{2} - 1\right) \quad (61)$$

The effect of ω on this bound is to cause it to move from the Γ_1 axis ($\Gamma_1 \leq -2$), its locus in Figure 3, to the left arm of the parabola for $l = 0$ in Figure 1 as ω increases from zero to infinity.

Thus an increasing heat capacity of the solid causes regions I and II of Figure 3 to contract, while the domain of complex eigenvalues, region III of Figure 3, increases.

The fact that the region of complex eigenvalues in the (Γ_1, Γ_2) plane increases in size does not necessarily imply that oscillations will be more prominent as the solid capacity increases. For given values of Γ_1 and Γ_2, it may be shown from Equations (56) and (57) that both the real and imaginary parts of λ become vanishingly small as ω increases to infinity. In fact as ω becomes very large even the real discrete eigenvalues approach zero as may be shown from Equation (53). Thus the dominant eigenvalues for a stable state are real, and any oscillatory contribution to the transient response might be unobservable for very large values of ω. For an unstable state, those eigenvalues with positive real parts will, of course, eventually dominate the transient response regardless of how small those eigenvalues are.

Consider next the locus of marginal oscillatory states, that curve which divides the domain of complex eigenvalues into stable and unstable regions. With $a = \pm b$ in Equations (56) and (57), the following parametric equations for this locus are obtained:

$$\Gamma_2 + \frac{8}{3}\omega|b|^3 = [(\Gamma_1 + 2) + 2|b|]^2 - 4b^2 \quad (62)$$

$$(\Gamma_1 + 2) + 2|b| = \frac{2}{3}\omega|b|\,(\Gamma_3 - |b| - 1) \quad (63)$$

In accordance with these relationships, Γ_1 is always less than -2 on the locus of marginal oscillatory states provided $\Gamma_3 < 1$. Furthermore, the locus moves in the (Γ_1, Γ_2) plane from the solid curve for $l = 0$ in the lower half of the plane in Figure 2 to the left arm of the parabola for $l = 0$ in Figure 1 as ω increases from zero to infinity. Thus as the solid heat capacity increases, the region of undamped oscillations (region III of Figure 3) disappears, and all unstable states become confined to the interior of the parabola for $l = 0$ shown in Figure 1.

In the case of a negligible thermal conductivity considered in the previous section, it was pointed out that no complex eigenvalues were possible for an adiabatic surface. In the present case it can be shown from Equation (58) that the locus of steady state solutions for $Q = 0$ given by Equation (51) will extend into the domain of complex eigenvalues in the (Γ_1, Γ_2) plane if $\Gamma_3 > 3/\omega$.

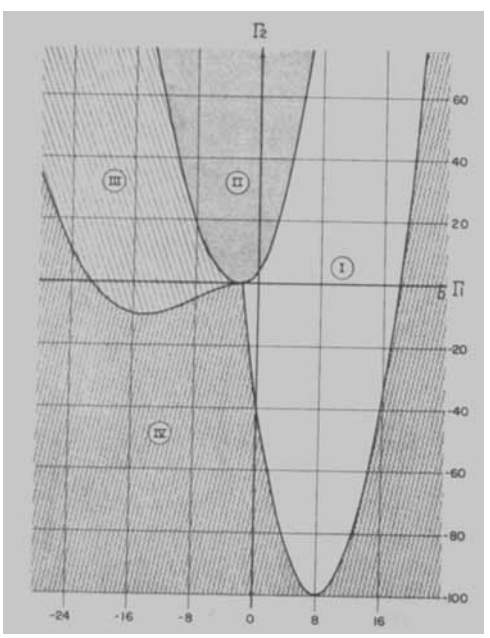

Fig. 4. Stability results for large solid conductivity with $\omega = 1$ and $\Gamma_3 = -1$.

Results of the considerations in this section are summarized in Figures 4 and 5. Figure 4 characterizes the transient features in the (Γ_1, Γ_2) plane for $\Gamma_3 = -1$ and $\omega = 1$. Each of the regions I, II, III, and IV in that figure has the same significance regarding the nature of transient state as the region designated by the same number in Figure 3. Figure 5 depicts the asymptotic situation as $\omega \to \infty$. These results verify the statement made earlier that conditions (43) and (50), which were derived for $\Gamma_4 = 0$, provide sufficient conditions for stability in the present case. Thus for $k_t^*/k_t \to \infty$, the transient description varies from that represented by Figure 3 to that by Figure 5, and ω covers the range of zero to infinity.

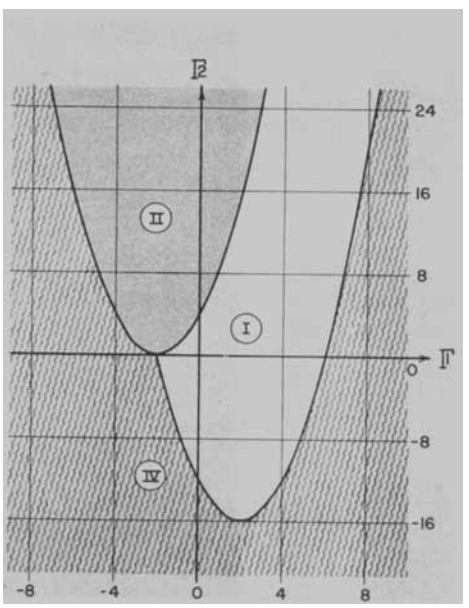

Fig. 5. Stability results for large solid conductivity with $\omega \to \infty$ and $\Gamma_3 = -1$.

Numerical computations have shown that region III is practically eliminated for $\omega > 40$ with $\Gamma_3 = -1$, and that region I reaches its asymptotic size shown in Figure 5 for $\omega > 100$. If the external fluid is taken to be air at 1 atm., ω for typical solid properties seems to be at least as large as 100, although at elevated pressures it could be considerably smaller. The values of ω and k_t^* could be controlled and brought very close to zero in an experimental study of transient phenomena if an evacuated spherical shell were used for the reaction surface. In normal applications, however, ω would apparently be sufficiently large so that the region of unstable oscillations in the (Γ_1, Γ_2) plane would be quite small. Nevertheless, its possible existence is of theoretical interest, since other distributed parameter reaction systems, such as those involving homogeneous reactions, undoubtedly exhibit transient features similar to those discussed here and perhaps are not so strongly influenced by the heat capacity of extraneous material. Thus the possible significance of all unstable regions of Figure 3 is worthwhile exploring. This is carried out in the following section by means of a numerical example.

It is noted that ω would be considerably smaller than the values mentioned above (of the order of 0.3) if the external fluid has typical liquid properties. The results presented here, however, may not be meaningful for liquid systems, principally because of the assumption of a Lewis number of unity.

NUMERICAL EXAMPLE

An example system is chosen here for the purpose of illustrating the possible significance of unstable steady states. To facilitate the computations, all physical properties are taken to be constant and the heat capacities of the various components of the fluid phase to be equal and constant. The reaction is taken to be irreversible and of the form $A_1 \rightarrow A_2$, with a kinetic expression given by

$$R = -kcx_1 \exp(-E/T) \tag{64}$$

Heat losses from the particle surface are assumed to occur by radiation to the surroundings. Thus

$$Q = \frac{\sigma\epsilon R_o}{cD}(T^4 - T_\infty^4) \tag{65}$$

With the assumptions stated for this illustration and with substitution from Equations (64) and (65) into Equations (18), (37), and (38) the following expressions are obtained for Γ_1 and Γ_2:

$$\Gamma_1 = \frac{k}{D}\left[1 - \frac{E}{T_{s,p}^2}\frac{x_{1s,p}(-\Delta H)}{C_p}\right] R_o e^{-E/T_{s,p}} + 4R_o\left(\frac{\sigma\epsilon}{k_t}\right)T_{s,p}^3 \tag{66}$$

$$\Gamma_2 = \Gamma_1^2 - 16\left(\frac{k}{D}\right)\left(\frac{\sigma\epsilon}{k_t}\right)R_o^2 T_{s,p}^3 e^{-E/T_{s,p}} \tag{67}$$

The steady state quantities at the particle surface, $x_{1s,p}$ and $T_{s,p}$ in Equations (66) and (67), are obtained from the steady state forms of Equations (2) and (3). Under the assumptions stated above, the solution of the former with the boundary conditions given in Equations (8) and (9) yields the following relationship for $x_{1s,p}$ in terms of $T_{s,p}$:

$$x_{1s,p} = \frac{x_{1\infty}}{1 + R_o\left(\frac{k}{D}\right)\exp(-E/T_{s,p})} \tag{68}$$

Similarly, the steady state form of Equation (3) may be solved in terms of H_∞ and an unknown surface temperature. Substitutions for enthalpy in terms of temperature and for $x_{1s,p}$ from Equation (68) into the solution and subsequent consideration of the boundary condition in Equation (9) result in the following trancendental equation for $T_{s,p}$:

$$\left(\frac{\sigma\epsilon}{k_t}\right)R_o(T_{s,p}^4 - T_\infty^4) + (T_{s,p} - T_\infty) = \frac{\left(\frac{(-\Delta H)x_{1\infty}}{C_p}\right)\left(\frac{k}{D}\right)R_o e^{-E/T_{s,p}}}{1 + \left(\frac{k}{D}\right)R_o e^{-E/T_{s,p}}} \tag{69}$$

It is noted that the steady state solution is independent of the properties of the solid material; the steady temperature is constant at $T_{s,p}$ throughout the particle.

The parameters employed here in numerical computations involving Equations (67) through (70) are as follows:

$$\left.\begin{aligned} k/D &= 4.08 \times 10^7 \text{ cm.}^{-1} \\ E &= 18{,}500 \text{ °K.} \\ (-\Delta H)\,x_{1\infty}/C_p &= 4{,}720 \text{ °K.} \\ \sigma\epsilon/k_t &= 1.10 \times 10^{-8} \text{ cm.}^{-1} \text{ °K.}^{-3} \end{aligned}\right\} \tag{70}$$

The nature of the transient response to small disturbances will be examined here for the system described by the above constants by means of the information in Figure 3. It is recalled that that figure provides necessary and sufficient conditions for stability if the solid material has a negligible thermal conductivity or heat capacity and sufficient conditions for the case of a large conductivity. The qualitative effect of an appreciable solid heat capacity on the instabilities will follow from the discussions of the previous section.

It is worth noting that the numerical values listed above were chosen to correspond roughly to those involved in the oxidation of carbon. The first-order rate constants are those reported by Parker and Hottel (7). Thus, for the sake of definiteness, one might think of the results as describing in a very qualitative way the behavior of burning particles of carbon. The interpretation of the results, of course, is not so restricted. The parameters in Equation (70) could just as easily apply to a surface catalyzed reaction system. In any case it should be strongly emphasized that significance is ascribable only to the qualitative features of the results due to the simplifying assumptions involved.

By means of Equations (66), (67), and (68) the information regarding stability and oscillatory behavior presented in Figure 3 can be transferred readily to the $(T_{s,p}, R_o)$ plane. Figure 6 shows the resulting regions I, II, III, and IV in that plane which correspond to regions designated by the corresponding numerals in Figure 3. The mapping of the left arm of the parabola for $l = 0$ in Figure 1 is shown as the dashed curve in Figure 6. It follows from discussion in the previous section of the effect of the solid heat capacity that the states within the region enclosed by the dashed curve are unstable for a solid thermal conductivity of zero or infinity and that no other states are unstable if the solid heat capacity is very large.

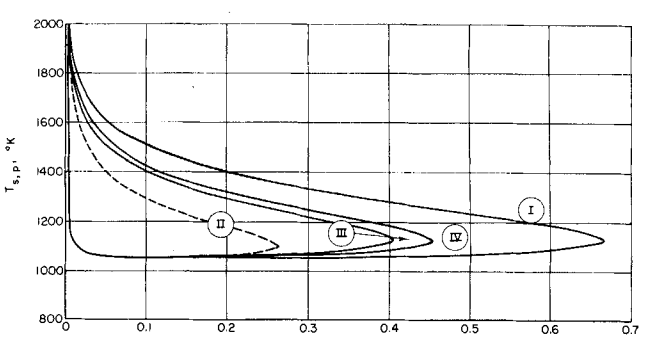

Fig. 6. Regions of instability and oscillatory behavior from Figure 3.

As is evident from the equations involved, the boundaries of the regions shown in Figure 6 are independent of T_∞. In fact that parameter has not yet been specified. Thus any point in the $(T_{s,p}, R_o)$ plane is a possible steady state solution for some value of T_∞. (There may be certain regions in the plane which are physically inaccessible because they would result only for a negative value of T_∞.)

Thus a family of steady state curves with T_∞ as a parameter resulting from solutions of Equation (69) could be superimposed on Figure 6. Such curves are shown in Figure 7. The dashed sections of the curves in that figure correspond to those sections which lie in regions II or III in Figure 6.

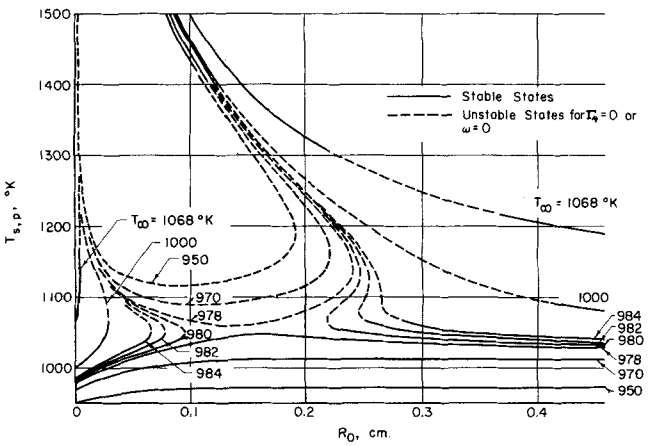

Fig. 7. Steady state solutions.

A number of interesting and significant features of these results merit discussion. First of all it is evident from Figure 7 that three distinct steady state solutions for the surface temperature may exist for some values of R_0. This is recognized as a common observation in theoretical studies of exothermic reaction systems of various types and has previously been pointed out specifically for exothermic reaction on spherical surfaces (*1, 2*). The three states are generally termed high, intermediate, and low temperature states or correspondingly high, intermediate, and low conversion states in view of their relative temperature or reaction-rate levels. In combustion applications the high and low temperature states are frequently referred to as *burning* and *extinguished* states, respectively. As also is evident from Figure 7, the intermediate state is always unstable. In fact, it can be shown by means of Equation (69) that the locus of points for which $dT_{s,p}/dR_0 = 0$ in Figure 7 is just coincident with the parabola shown in Figure 1 for $l = 0$. As a result, the intermediate state and only the intermediate state lies within that parabola. The region bounded by the dashed curve then in Figure 6 shows those values of R_0 for which there is a possibility of multiple states. As was pointed out earlier, all steady states in the case of an adiabatic surface lie along the curve given by Equation (51) and, as a result, are always confined to regions I and IV and the interior of the parabola for $l = 0$ in Figure 1. It may be concluded then that only the intermediate state can be unstable in an adiabatic case, and when a single steady state exists, it is stable.

The results in Figures 6 and 7 show that this is not necessarily the case for a nonadiabatic surface. Suppose for the moment that all dashed portions of the curves in Figure 7 represent unstable states, as indeed they do when solid conductivity or capacity are negligible. With $T_\infty = 950°K.$, as an example, the steady state curve in Figure 7 shows that for any particle radius between 0.107 and 0.192 cm. both the high and intermediate temperature states are unstable. For these sizes, then, only a low temperature, low conversion state could exist physically. Another interesting observation from Figures 6 and 7 is that the system may possess no stable state at all. For example, with $T_\infty = 982°K.$ and particle radii between 0.244 and 0.252 cm., three steady state solutions exist, but none are stable. In fact for $T_\infty = 982°K.$ no stable state exists for particle radii between 0.145 and 0.252 cm. In those cases where no stable state exists, the system would be expected to oscillate continuously in time, since concentrations and temperature must remain bounded.

It follows from earlier discussions that with a large solid thermal conductivity the effect of an appreciable solid heat capacity would be to reduce the magnitudes of unstable regions II and III in Figure 6. In most realistic situations, region III may be virtually eliminated and region II practically shrunk to the dashed curve of Figure 6. Some of the phenomena described above then would be possible only on very narrow ranges of conditions and might have little practical significance.

The pattern of steady state multiplicity shown in Figure 7 is itself interesting. For a number of values of T_∞ shown, the region of multiplicity disappears as R_0 is increased and then reappears at larger values of R_0. This phenomenon must be due to the relative effects of R_0 on heat losses by radiation and heat generation by chemical reaction.

Although the model here is not applicable to systems of particles unless a single particle has no near neighbor, one may conjecture, from the results shown in Figure 7, the assortment of behavior that may be observable in a system of particles with a distribution of sizes at a fixed value of T_∞.

The results shown in Figure 7 may have additional significance regarding the prediction of extinction conditions in combustion processes. Traditionally that theory has been based solely on steady state results. Some recent studies (*8, 9*) have illustrated the possibility of errors in this interpretation. To illustrate this possibility, assume again that all dashed portions in Figure 7 are unstable, although it is now acknowledged that the effects of instabilities are quantitatively exaggerated by this assumption. To cite one particular example, a particle of radius 0.220 cm. would, in accordance with traditional theory, be extinguished if T_∞ were decreased just below 970°K. because for lower values only an extinguished steady state exists. However, Figure 7 shows that for T_∞ below 1,068°K., no stable burning steady state is possible; unstable burning states are physically unrealizable. Thus if the ambient temperature were continually decreased in a system containing a particle of this radius, steady high temperature, high conversion performance would be observed for $T_\infty > 1{,}068°K.$ As T_∞ is decreased just below 1,068°K., situations are first encountered in which a single, unstable steady state exists. As mentioned earlier, sustained oscillatory behavior would be expected in these cases. Further decreases in T_∞ to values below 980°K. lead to situations in which three steady states exist, but only the relatively low temperature or extinguished state is stable. This is depicted for example by curves for 978°K. in Figure 7. In such cases wherein a stable steady state exists, the system would probably seek that state, and if so, the burning process would be extinguished at about 980°K. in the above example. There is the possibility that the state of the system would oscillate continuously about the unstable high temperature instead of proceeding to a stable point. Though such behavior seems unlikely and is known not to occur in lumped reaction systems, it apparently cannot be ruled out theoretically in the present distributed problem unless nonlinear effects are taken into account.

As was pointed out earlier, only the intermediate state is unstable to small disturbances in the case of an adiabatic surface. It follows then that the traditional theory of extinction is valid in such cases. However, since no real system is completely free from heat losses, extinc-

tions should probably be considered to be the result of instabilities rather than the result of the sensitivity of steady state solutions to parameter changes. The effect of the solid heat capacity would apparently cause little difference in conditions at the two types of extinction in most cases.

SUMMARY

Linear stability theory has been applied to a nonisothermal system involving a surface reaction on a single spherical particle. Necessary and sufficient conditions for stability have been derived for the limiting cases of zero and infinite solid thermal conductivity.

The results of the analysis show that nonadiabaticity of the solid surface could possibly lead to certain unstable behavior, such as undamped oscillatory responses, which is characteristically different from that for adiabatic surfaces. It is shown, however, that such behavior is practically eliminated when the solid heat capacity is large and would seem to be of little significance owing to the solid capacity effect in most realistic cases. Nevertheless, the possible unstable behavior is of theoretical interest.

An example system involving a first-order exothermic reaction was studied numerically to illustrate the possible occurrence of instabilities as well as their significance, particularly regarding the prediction of extinction conditions in particle burning.

ACKNOWLEDGMENT

This study received financial support through a grant from the Army Research Office, Durham, and from a DuPont Grant-in-Aid. Fellowships for D. K. Winegardner from the American Oil Company and Union Carbide are also acknowledged.

NOTATION

a, $|a|$ = real part of λ and absolute value of the real part
$\bar{a}$ = real part of λ
$\mathbf{a}$, a_j = vector of stoichiometric coefficients and its j^{th} component
$\mathbf{A}$ = matrix defined in Equation (18)
A_j = chemical species
b, $|b|$ = imaginary part of λ and absolute value of the imaginary part
$\bar{b}$ = imaginary part of λ
$\mathbf{B}$ = matrix defined in Equation (19)
c = mass or molar density of fluid
C_p, C_p^* = fluid and solid heat capacities
C_{pj} = heat capacity of component A_j
$\mathbf{C}$ = matrix defined in Equation (20)
$\det(\mathbf{J})$ = determinant of the matrix $\mathbf{J}$
D = diffusivity in the fluid
E = activation energy divided by gas constant
$\mathbf{f}$ = vector of eigenfunctions in Equation (21)
f^* = eigenfunction in Equation (21)
h_j = partial enthalpy of component A_j relative to its atomic form
H = enthalpy per unit mole or unit mass of fluid mixture
ΔH = enthalpy of reaction, $= -\sum_{j=1}^{n} a_j h_j^o$
$\mathbf{I}$ = identity matrix
I_ν = modified Bessel function of order ν
$Im(z)$ = imaginary part of complex quantity z
k = pre-exponential factor in surface kinetic expression
k_t, k_t^* = fluid and solid thermal conductivities
l = wave number for θ
L = ratio of solid to fluid thermal diffusivities
m = wave number for ϕ
n = number of components in mixture
p, p^* = perturbation variables defined in Equations (12) and (13)
$p_l^m(\cos\theta)$ = associated Legendre polynomial
Q = heat loss function defined in Equations (8) and (65)
r = radial variable measured from center of spherical particle
R = dimensionless intrinsic reaction rate, $\mathcal{R}\, R_o/cD$
$\mathcal{R}$ = intrinsic rate of formation per unit area of surface
R_o = particle radius
$Re(z)$, $|Re(z)|$ = real part of complex quantity z and absolute value of the real part
t = time
$tr(\mathbf{J})$ = trace of matrix $\mathbf{J}$
T, T^* = absolute temperatures of fluid and solid
v = function defined in Equation (37)
V = function defined is Equation (36)
$\mathbf{x}$, x_j = vector of mole or mass fraction and its j^{th} component

Greek Letters

α, β = vectors of constants in Equation (27)
α^*, β^* = constants defined in Equation (28)
Γ_1, Γ_2, Γ_3, Γ_4 = functions defined in Equations (37), (38), (39), and (40)
∇^2 = Laplacian operator in spherical coordinates
ϵ = emissivity for radiative heat loss
η = dimensionless radial variable, r/R_o
θ = angular variable
λ = eigenvalue in Equation (21)
ρ^* = density of the solid
σ = Boltzmann radiation constant
τ = dimensionless time, tD_∞/R_o^2
ϕ = angular variable
ω = $\rho^* C_p^*/cC_p$

Subscripts

∞ = condition at infinite distance from solid surface
p = particle surface
s = steady state

Superscripts

o = reference state
$'$ = differentiation with respect to η

LITERATURE CITED

1. Petersen, E. E., J. C. Friedly, and R. J. DeVogelaere, *Chem. Eng. Sci.*, **19**, 683 (1964).
2. Petersen, E E., and J. C. Friedly, *ibid.*, 783.
3. Amundson, N. R., and L. R. Raymond, *AIChE J.*, **11**, 339 (1965).
4. Kuo, J. C. W., and N. R. Amundson, *Chem Eng. Sci.*, **22**, 49 (1967).
5. Dettman, J. W., "Mathematical Methods in Physics and Engineering," McGraw-Hill, New York (1962).
6. Abramowitz, Milton, and Irene A. Stegun, ed., "Handbook of Mathematical Functions," U.S. Government Printing Office, Washington, D.C. (1965).
7. Parker, A. S., and H. C. Hottel, *Ind. Eng. Chem.*, **28**, 1334 (1936).
8. Schmitz, R. A., and M. P. Grosboll, *Combustion and Flame*, **9**, 340 (1965).
9. Kirkby, L. L., and R. A. Schmitz, *ibid.*, **10**, 205 (1966).

Manuscript received September 15, 1966; revision received May 22, 1967; paper accepted June 26, 1967.